ARL-TR-8497 ● SEP 2018

US Army Research Laboratory

Photo, Thermal, and Temporal Stability of Protein-Templated Fluorescent Gold Nanoclusters

by Sasha Teymorian, Lily Giri, Joseph R Palmeri, Andres A Bujanda, and Shashi P Karna

NOTICES

Disclaimers

The findings in this report are not to be construed as an official Department of the Army position unless so designated by other authorized documents.

Citation of manufacturer's or trade names does not constitute an official endorsement or approval of the use thereof.

Destroy this report when it is no longer needed. Do not return it to the originator.

ARL-TR-8497 ● SEP 2018

US Army Research Laboratory

Photo, Thermal, and Temporal Stability of Protein-Templated Fluorescent Gold Nanoclusters

by Sasha Teymorian, Andres A Bujanda, and Shashi P Karna
Weapons and Materials Research Directorate, ARL

Lily Giri
SURVICE Engineering, 4694 Millennium Dr, Belcamp, MD

Joseph R Palmeri
ARL College Qualified Leader Program Participant

REPORT DOCUMENTATION PAGE

Form Approved
OMB No. 0704-0188

1. REPORT DATE *(DD-MM-YYYY)*	2. REPORT TYPE	3. DATES COVERED (From - To)
September 2018	Technical Report	April 2017–March 2018

4. TITLE AND SUBTITLE
Photo, Thermal, and Temporal Stability of Protein-Templated Fluorescent Gold Nanoclusters

5a. CONTRACT NUMBER

5b. GRANT NUMBER

5c. PROGRAM ELEMENT NUMBER

6. AUTHOR(S)
Sasha Teymorian, Lily Giri, Joseph R Palmeri, Andres A Bujanda, and Shashi P Karna

5d. PROJECT NUMBER

5e. TASK NUMBER

5f. WORK UNIT NUMBER

7. PERFORMING ORGANIZATION NAME(S) AND ADDRESS(ES)
US Army Research Laboratory
Weapons and Materials Research Directorate (ATTN: RDRL-WM)
Aberdeen Proving Ground, MD 21005-5066

8. PERFORMING ORGANIZATION REPORT NUMBER
ARL-TR-8497

9. SPONSORING/MONITORING AGENCY NAME(S) AND ADDRESS(ES)

10. SPONSOR/MONITOR'S ACRONYM(S)

11. SPONSOR/MONITOR'S REPORT NUMBER(S)

12. DISTRIBUTION/AVAILABILITY STATEMENT
Approved for public release; distribution is unlimited.

13. SUPPLEMENTARY NOTES

14. ABSTRACT

Biotemplated fluorescent gold nanoclusters (AuNCs) have received a great deal of attention due to their ultra-small size, biocompatibility, and tunable fluorescent properties. Of particular interest are protein-templated gold nanoclusters (P-AuNCs), many of which have been shown to combine the photophysical properties of AuNCs as well as the native bioactivity of proteins. Although there is substantial research on the synthesis of biostabilized AuNCs, there are few reports on the photostability and thermal stability of these AuNCs. This report examines the photostability and thermal stability of bioconjugated P-AuNCs using two different protein templates: bovine serum albumin (BSA) and pepsin. The red-emitting BSA-AuNCs and the green-emitting pepsin-AuNCs exhibited resistance to photobleaching under continuous UV irradiation (λ = 365 nm) for up to 24 h; the blue-emitting pepsin-AuNCs were nearly twofold less photostable. Interestingly, the blue-emitting NCs exhibited the greatest thermal stability, retaining approximately 80% of their initial fluorescence intensity after 30-min incubation at 80 °C, while the BSA-AuNCs retained approximately 30% of their initial fluorescence, and the pepsin-AuNCs lost all fluorescence due to protein precipitation out of solution. All three synthesized P-AuNCs exhibited minimal loss (less than 10%) in fluorescence intensity for a period of up to 6 months when stored at 4 °C. These results suggest the robustness and enhanced thermal and photostability of P-AuNCs, making them highly attractive for a wide range of optoelectronics, sensing, and imaging applications.

15. SUBJECT TERMS
metal nanocluster materials, protein-templated, transmission electron microscopy, TEM, photostability, thermal stability

16. SECURITY CLASSIFICATION OF:			17. LIMITATION OF ABSTRACT	18. NUMBER OF PAGES	19a. NAME OF RESPONSIBLE PERSON
a. REPORT	b. ABSTRACT	c. THIS PAGE			Sasha Teymorian
Unclassified	Unclassified	Unclassified	UU	24	19b. TELEPHONE NUMBER (Include area code) (410) 306-4787

Contents

List of Figures

Acknowledgments

This research at the US Army Research Laboratory was partly supported by funding from the Medical Research and Materials Command. The research by Joseph R Palmeri was supported by the College Qualified Leaders program of the US Army Education Outreach Program. Sasha Teymorian would like to thank J Derek Demaree for assistance with X-ray photoelectron spectroscopy data interpretation and figure generation.

1. Introduction

Gold nanoclusters (AuNCs) have attracted a great deal of attention because of their unique photophysical and physiochemical properties.[1–4] Ranging in size from fewer than 10 to several hundred atoms (2 nm or less), AuNCs possess discrete energy levels and exhibit size-tunable fluorescence emissions. In addition, fluorescent AuNCs exhibit a high degree of biocompatibility and do not disturb biological functions or labeled bioentities.[5–13] These properties make AuNCs highly attractive for biolabeling and bioimaging applications.[14–18]

Among the several synthetic methods developed recently for preparing AuNCs in solutions, protein-directed synthesis has gained attention due to its biocompatibility, environmental friendliness, and mild reaction conditions.[18–27] Xie et al. first demonstrated the synthesis of red-fluorescent AuNCs using bovine serum albumin (BSA), the most abundant plasma protein in cows and which is widely used in biosensing and boimaging to sequester and reduce Au precursors in situ.[27] Since then, several other proteins including pepsin,[3] lysozyme,[28] insulin,[29] human transferrin,[10] horseradish peroxidase (HRP),[30] and Deoxyribonuclease I (DNAseI)[31] have been used as templates to synthesize AuNCs. Interestingly, some proteins (HRP and DNAseI) have been shown to retain their native functions while bioconjugated to the AuNCs, thus offering a multifunctional bio-nano hybrid system capable of simultaneous detection and quantification of targeted biological processes.[10,25,31–35]

Although a variety of biostabilized AuNC conjugates have been synthesized, the formation and stabilization mechanisms of AuNCs in protein conjugates remain a topic of investigation. Numerous reports have suggested that the diversity in amino acid (aa) content in protein templates and the size (kiloDaltons [kDa]) of the protein influence AuNC formation and properties.[5,35–41] Studies have shown that the charge transfer ability of the surface ligands to the Au core play a major role in fluorescence: electron-rich atoms (such as oxygen [O] and nitrogen [N_2]) or functional groups in the protein molecules surrounding the Au core can effectively enhance fluorescence via surface interactions.[35] Additionally, the balance of amine-containing amino acids, which are responsible for Au ion uptake, and the ratio of tyrosine to tryptophan aa residues [responsible for the reduction of Au(III) to Au(I)] within a protein are critical for NC formation.[35,36,38] Furthermore, the number of cysteine (cys) residues has been linked to AuNC formation because of the stability provided by the strong interaction between Au and thiol groups.[35,36,38] However, AuNCs have been biosynthesized using myoglobin, an iron- and oxygen-binding protein found in muscle cells, which contains no cys residues. The myoglobin-stabilized AuNCs exhibited a blue shift in fluorescence emission,

suggesting that the number of cys residues may play a role in the emission wavelength of fluorescent AuNCs.[38,42]

To date, reports on the photostability and thermal stability of these P-AuNCs have been limited. These are important properties to understand and develop for the use of P-AuNCs in bioimaging, disease diagnosis, and, as some P-AuNCs retain their biological role, as potential targeted drug-delivery systems. Herein we report the resistance of red-emitting BSA-, green-emitting pepsin-, and blue-emitting pepsin-P-AuNCs to photobleaching as a function of continuous UV irradiation. In addition, we report the thermal stability of the three P-AuNCs as measured by monitoring fluorescence intensity after incubation at high temperatures. All three P-AuNCs exhibited intense fluorescence emission, resistance to photobleaching, high thermal stability, and long-term stability in solution and in dried form.

2. Materials and Methods

BSA and pepsin proteins were purchased as lyophilized powders from Sigma Aldrich and used directly without further purification. Au(III) chloride trihydrate powder was purchased from Sigma Aldrich. Conductive silicon (Si) and nonconductive Si/silicon dioxide (SiO_2) wafers were purchased from Nova Electronic Materials and cleaned prior to use as follows: 20-min sonication in acetone to remove any debris from the wafer surface, followed by an ethanol rinse and a Milli-Q water rinse, and finally dried with N_2 gas. Transmission electron microscopy (TEM) grids (ultrathin carbon film on holey carbon support film, 300 mesh) were purchased from Ted Pella, Inc. Quartz glass cuvettes (700 µL) for fluorescence measurements were purchased from Thorlabs. All solutions were prepared fresh to working concentrations in ultrapure Milli-Q water; P-AuNC solutions were prepared in triplicate, and fluorescence measurements were recorded in triplicate and averaged.

2.1 BSA-AuNC Synthesis

BSA-stabilized AuNCs were prepared according to Xie et al.[27] Briefly, aqueous $HAuCl_4$ solution (5 mL, 10 mM) was added to BSA solution (5 mL, 50 mg/mL) under vigorous stirring at 37 °C. The control solution contained Milli-Q water (5 mL) and BSA solution (5 mL, 50 mg/mL). After 2 min, sodium hydroxide (NaOH) solution (0.5 mL, 1 M) was added to raise the pH to approximately 12 to activate the reduction ability of BSA [adjusting the reaction pH above the acid strength (pKa) of tyrosine (~10) enables the hydroxyl groups of the phenol ring to reduce Au(III) ions]. The mixture was then incubated under vigorous stirring at 37 °C for 12 h.

2.2 Green-Emitting Pepsin-AuNC and Blue-Emitting Pepsin-$Au_{5/8}$NC Synthesis

Green-emitting pepsin-stabilized AuNCs (green pepsin-AuNCs) were prepared according to Kawasaki et al.[3] Briefly, aqueous $HAuCl_4$ solution (0.5 mL, 5 mM) was added to pepsin solution (5 mL, 40 mg/mL) under vigorous stirring at 37 °C. The control solution contained Milli-Q water (5 mL) and pepsin solution (5 mL, 40 mg/mL). After 5 min, hydrochloric acid solution (0.3 mL, 1 M) was added to lower the pH to approximately 1. The mixture was then incubated under vigorous stirring at 37 °C for 100 h, followed by centrifugation at 4,000 rpm for 20 min to remove any aggregated pepsin-Au structures from the bioconjugate solution.[43] The green pepsin-AuNC–containing supernatant was stored at 4 °C until use.

To prepare the blue-emitting pepsin-stabilized AuNCs (blue pepsin-AuNCs), NaOH solution (1.0 mL, 1 M) was added to an aliquot of the green pepsin-AuNC supernatant solution to adjust the pH to approximately 9. The pH of the green pepsin-AuNC control solution was similarly adjusted to a pH of approximately 9 and used as the blue pepsin-AuNC control. The mixture was incubated at 37 °C for 1 day, followed by centrifugation at 4,000 rpm for 20 min. The blue pepsin-AuNC-containing supernatant was stored at 4 °C until use.

2.3 Fluorescence of BSA-AuNC, Green Pepsin-AuNCs, and Blue Pepsin-AuNCs in Aqueous Solution and in Dried Form

The fluorescence emission spectra of the aqueous P-AuNC solutions were collected using a Horiba Jobin Yvon FluoroLog-3 spectrofluorometer with maximum excitation wavelengths of 330 and 480 nm. The emission spectra was measured from 360 to 800 nm.

To observe fluorescence of the P-AuNCs in the dried form, aliquots (25 µL) of P-AuNCs in solution were drop-cast onto cleaned Si and Si/SiO_2 wafers (1.0 cm × 1.0 cm), and dried at 37 °C for 2 h. The fluorescence of the dried samples was verified under UV lamp (λ = 365 nm).

2.4 Transmission Electron Microscopy

TEM micrographs of protein-NC conjugates were collected using a JEOL JEM-2100F TEM/scanning TEM instrument, operated at 200 kV. Aliquots (10 µL) of P-AuNCs were drop-cast onto TEM grids, and excess solution drawn out using filter paper. The grids were allowed to dry at room temperature (RT) for 1 h.

2.5 X-Ray Photoelectron Spectroscopy (XPS) Analysis

XPS analysis was performed using PHI 5000 VersaProbe II with a 100-W monochromatic aluminum Kα (1,486.7 eV) X-ray source, which irradiated a 200- × 200-µm sampling area with a takeoff angle of 45°. The XPS chamber base pressure was 7.2×10^{-8} Pa; elemental high-resolution scans for Au_{4f} core level were taken with 23.5-eV pass energy. The sp^3 C_{1s} peak at 285 eV was used as reference for binding energy calibration. Aliquots (25 µL) of P-AuNC were drop-cast onto Si wafers (0.5 × 0.5 cm) and allowed to dry at 37 °C for 2 h.

2.6 BSA-AuNC, Green Pepsin-AuNCs, and Blue Pepsin-AuNCs Resistance to Photobleaching

The photostability of the P-AuNCs was examined as a function of constant UV irradiation (λ = 365 nm) using a Blak-Ray B-100A High Intensity UV Lamp (UVP ChemStudio, Upland, CA). Samples were prepared as previously described, and fluorescence measurements were taken at timed intervals for up to 24 h.

2.7 Thermal Stability

Aliquots (0.8 mL) of the P-AuNCs in solution were added to 1.5-mL microcentrifuge tubes and incubated for 30 min in an Eppendorf Thermomixer C at 10 °C intervals from 40 to 100 °C. Control samples were incubated at RT (25 °C) for 30 min. Fluorescence was measured immediately following incubation. To investigate the ability of the P-AuNCs to renature after thermal denaturation, samples were allowed to recover at RT for 2 h and fluorescence measured.

3. Results and Discussion

3.1 Fluorescence of Aqueous BSA-AuNC, Green Pepsin-AuNC, and Blue Pepsin-AuNC Solutions

The color of the BSA-AuNC solution changed from a light golden yellow at the start of the reaction to a deep reddish gold upon completion (Fig. 1A, top). The BSA-AuNC solution emitted an intense red fluorescence (Fig. 1A, bottom) under UV light (λ = 365 nm). In contrast, the control solution was pale yellow under visible light (Fig. 1A, top) and emitted a weak blue fluorescence under UV light (Fig. 1A, bottom). This weak blue emission is due to the aromatic aa residues (major contribution from tryptophan) in the protein. The BSA-AuNCs showed excitation and emission peaks at 480 and 640 nm (Fig. 1B), respectively. The intense red fluorescence of the BSA-AuNCs was retained with minimal loss (less than 10% of initial fluorescence intensity) throughout the 6 months measured when stored at 4 °C (data not shown).

The green pepsin-AuNCs emitted an intense green fluorescence (Fig. 1A, bottom) under UV light (λ = 365 nm) and showed excitation and emission peaks at 330 and 510 nm (Fig. 1B), respectively. In contrast, the control solution was pale yellow under visible light and emitted a weak blue fluorescence under UV light (data not shown). The blue pepsin-AuNCs emitted an intense blue fluorescence (Fig. 1A, bottom) under UV light, and showed excitation and emission peaks at 330 and 402 nm (Fig. 1B), respectively. In contrast, the control solution was pale yellow under visible light and emitted a weak blue fluorescence under UV light (data not shown). The intense green and blue fluorescence of the pepsin-AuNCs was retained with minimal loss (less than 10% of initial fluorescence intensity) throughout the 6 months measured when stored in solution at 4 °C (data not shown). The size range for the overall protein-AuNCs and the cluster alone are expected to be 4-6 nm and 1-2 nm, respectively, however this was not a focus of the current study.

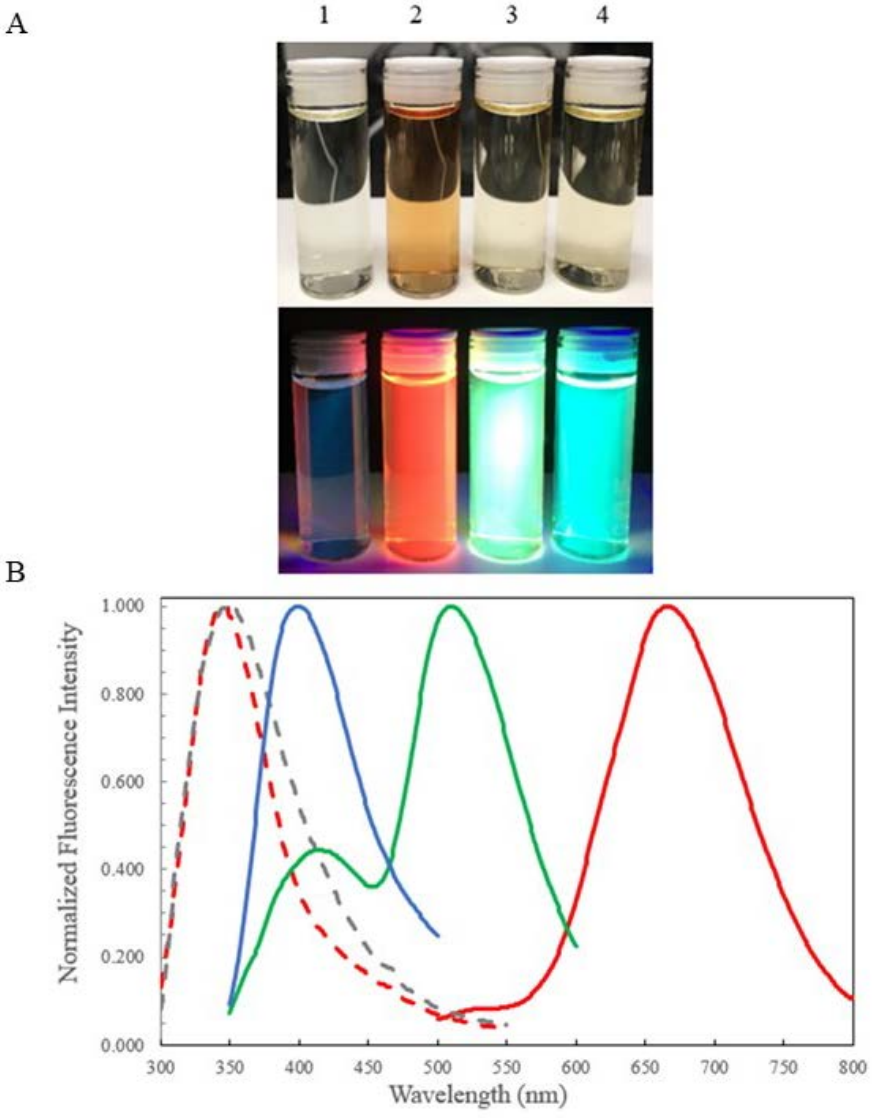

Fig. 1 A) Photographs of size-tunable fluorescence of BSA- and pepsin-AuNCs under visible (top) and UV (bottom) light: 1) BSA control solution; 2) BSA-AuNCs; 3) green-emitting pepsin-AuNCs; and 4) blue-emitting pepsin-AuNCs. B) Fluorescence emissions spectra of aqueous solutions of red BSA-AuNCs (solid red), green pepsin-AuNCs (solid green), and blue pepsin-AuNCs (solid blue). Fluorescence emissions of BSA control solution (dashed red) and pepsin control solution (dashed gray) are also shown.

Whereas the fluorescence intensity of the synthesized P-AuNCs in solution is important for design of biological sensors and in bioimaging, the fluorescence intensity in the dried form is important for optoelectronic applications. Therefore, fluorescence emissions of the BSA- and pepsin-AuNCs were examined under visible (Fig. 2, top) and UV (Fig. 2, bottom) light. The data show each protein cluster retains intense fluorescence in the dried form (Fig. 2), indicating the stability of the P-AuNCs. Fluorescence was retained throughout the 6 months measured (data not shown).

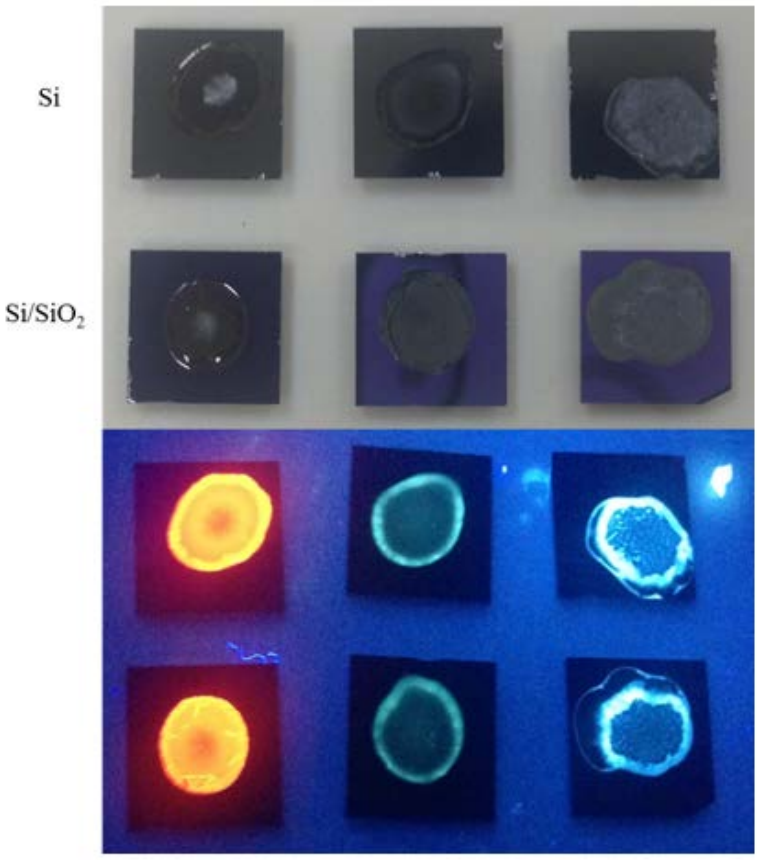

Fig. 2 (top) Fluorescence emission from red BSA-AuNC (red), green pepsin-AuNC (green), and blue pepsin-AuNC (blue) on Si and Si/SiO2 substrates. Aliquots (25 µL) of P-AuNCs were drop-cast onto cleaned wafers and allowed to dry at 37 °C for 2 h. (bottom) Fluorescence was verified under UV lamp (λ = 365 nm).

3.2 Physical Properties of BSA-AuNC, Green Pepsin-AuNCs, and Blue Pepsin-AuNCs

The size and oxidation states of the BSA- and pepsin-NCs were characterized using high-resolution (HR) TEM and XPS. The HR-TEM micrographs of BSA-AuNC show agglomeration of the protein-NCs, ranging from 1 to 3 nm in size (Fig. 3A). No clear image of the pepsin-AuNCs were obtained possibly due to 1) degradation of the sample under the electron beam; the beam may have condensed on the specimen, causing it to "burn" (data not shown),[44] or 2) the bioconjugated clusters being too small to be visible under TEM observation.

The $Au_{4f7/2}$ XPS peak for each P-AuNC was examined to determine cluster size. The Au(0) peak, corresponding to bulk Au, is centered at approximately 84 eV; the Au(I) peak, corresponding to surface Au, is centered at approximately 86 eV. Both peaks contribute to the overall $Au_{4f7/2}$ peak shape. The XPS spectra for BSA-AuNCs shows the $Au(0)_{4f\,7/2}$ peak is centered mainly at approximately 84 eV, with some asymmetry due to minor Au(I) contribution (Fig. 3B). The XPS spectra for green pepsin-AuNC reveals a peak shift to higher energies (approximately 85 eV) because the Au(I) contribution is greater, a result of higher levels of surface Au in smaller clusters (Fig. 3B). The signal for the blue pepsin-AuNCs is weak, possibly due to the very small cluster size. Zooming in on the blue pepsin-AuNC spectra reveals that the Au(I) contribution is large (a result of the very small cluster size); therefore, separate peaks for Au(I) and Au(0) are resolved (Fig. 3B). Thus, the XPS data suggest the following order, from largest to smallest, for P-AuNC size: BSA-AuNC > green pepsin-AuNCs > blue pepsin-AuNCs. This order is confirmed by the measured fluorescence emission wavelengths (Fig. 1).

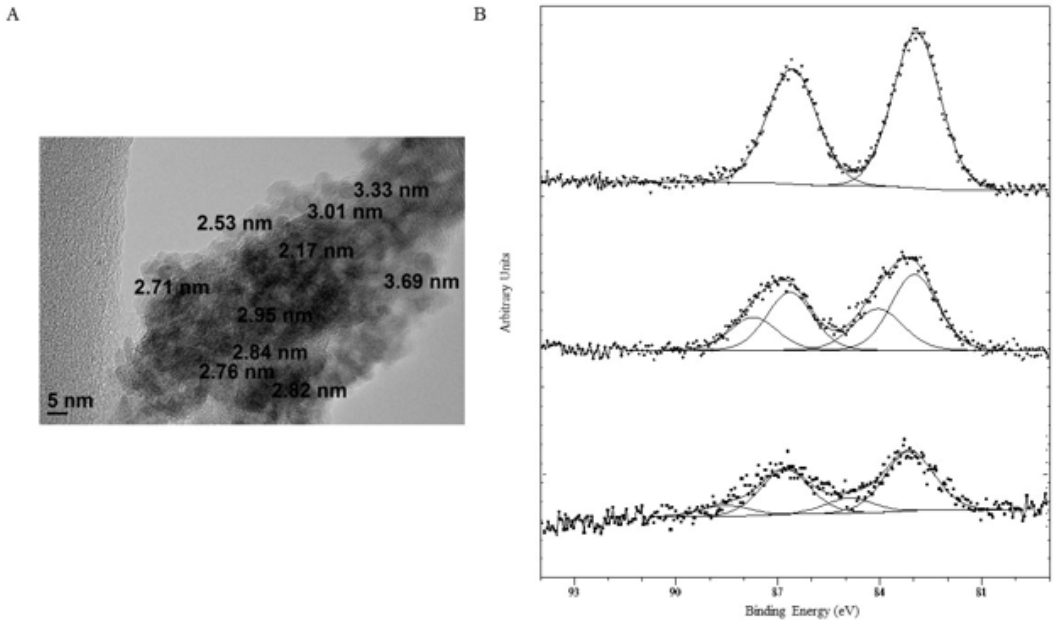

Fig. 3 A) High-resolution TEM image of BSA-AuNC, revealing the presence of NCs 1–3 nm in size. Aliquots (10 µL) of P-AuNCs were drop-cast onto TEM grids and excess solution drawn out with filter paper. The grids were allowed to dry at RT for 1 h. B) XPS spectra of red BSA-AuNC (top spectrum), green pepsin-AuNC (middle spectrum), and blue pepsin-AuNC (bottom spectrum) on Si wafers. Aliquots (25 µL) of P-AuNCs were drop-cast onto cleaned Si wafers and allowed to dry at 37 °C for 2 h.

3.3 Photostability of BSA-AuNC, Green Pepsin-AuNCs, and Blue Pepsin-AuNCs

The photostability of the BSA- and pepsin-AuNCs were examined as a function of constant UV irradiation (λ = 365 nm) for up to 24 h. The data reveal that the red-fluorescent BSA-AuNCs and green pepsin-AuNCs exhibit a more gradual rate of photobleaching than the blue pepsin-AuNCs (Fig. 4). After 24 h of constant UV exposure, the BSA-AuNCs and green pepsin-AuNCs retained approximately 60% and approximately 50% of their initial fluorescence intensity, respectively, whereas the blue pepsin-AuNCs retained approximately 10% of their initial fluorescence intensity. These data indicate the greater photostability of the BSA-AuNCs, which may originate from more-complete coverage of the surface Au atoms by the large size of the protein template (636 aa compared with 327 aa in pepsin) and potential formation of six Au-thiol surface motifs originating from the 18 thiol groups of BSA.[38]

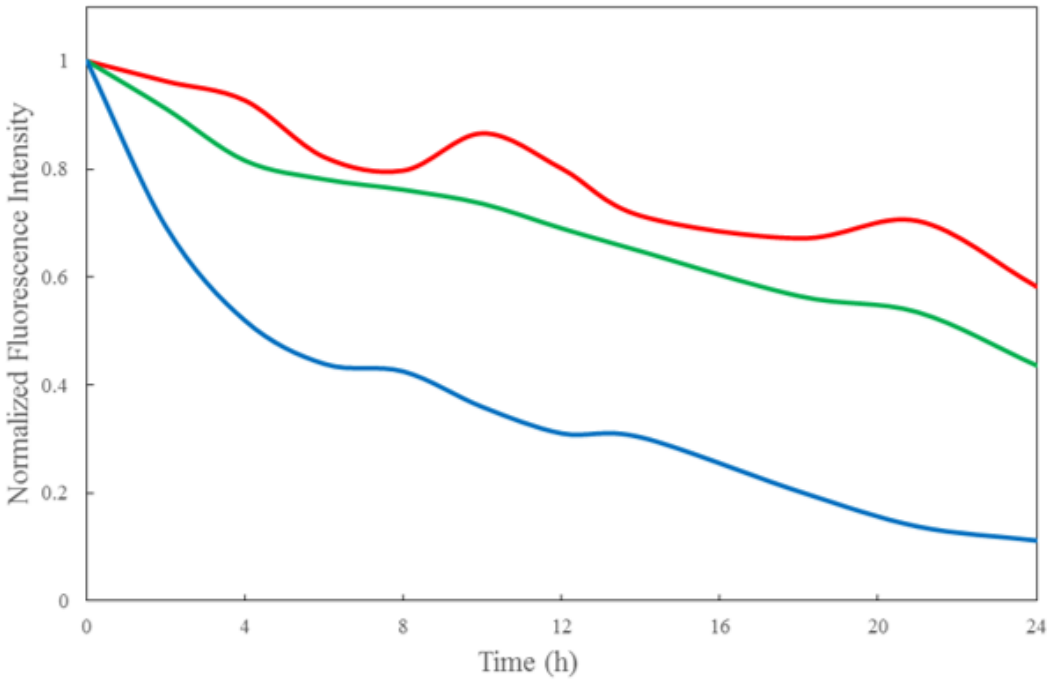

Fig. 4 Normalized fluorescence intensity of red BSA-AuNC (red), green pepsin-AuNC (green), and blue pepsin-AuNC (blue) as a function of constant UV irradiation (λ = 365 nm) for up to 24 h

3.4 Thermal Stability of Red BSA-AuNCs, Green Pepsin-AuNCs, and Blue Pepsin-AuNCs in Solution

The thermal stability of the BSA- and pepsin-AuNCs in solution was examined by monitoring the fluorescence intensity after a 30-min incubation at temperatures ranging from 40 to 100 °C and by comparing the intensities with that of the control P-AuNCs, which were incubated for 30 min at RT (25 °C). Figure 5 shows the normalized fluorescence intensity of each P-AuNC solution at the selected representative temperatures across the assayed range: 25, 60, 80, and 100 °C. For comparison, native BSA and pepsin begin to denature (unfold and aggregate) at 65 and 55 °C, respectively.

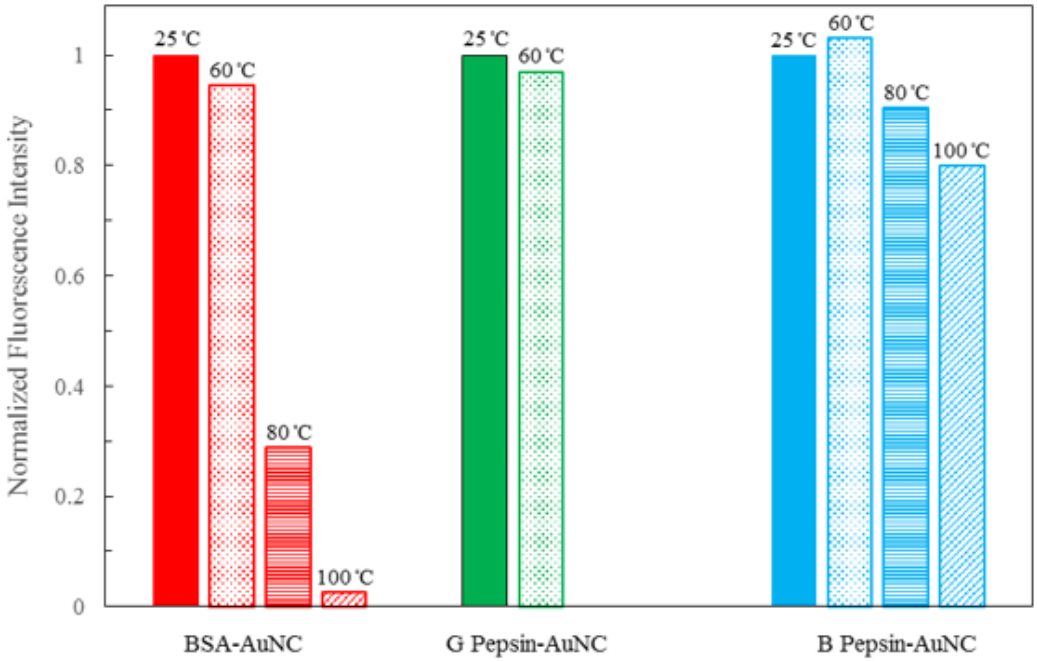

Fig. 5 Thermal stability of BSA- and pepsin-AuNCs in solution. Aliquots (800 µL) of P-AuNCs were incubated for 30 min from 40 to 100 °C at 10 °C intervals. Control P-AuNC solutions were incubated for 30 min at 25 °C. Fluorescence measurements were taken immediately after incubation.

Overall, the fluorescence intensities of all three P-AuNCs decreased as the temperature increased. At 60 °C incubation, all three P-AuNC samples retained fluorescence levels similar to that of the corresponding control sample. At 80 °C, BSA-AuNCs and blue pepsin-AuNCs retained approximately 30% and approximately 90%, respectively, of the fluorescence intensity of the controls (see Fig. 5). In contrast, the protein of the green pepsin-AuNCs precipitated out of the solution at 80 °C and fluorescence was lost. At 100 °C, the BSA-AuNCs retained approximately 5% of the fluorescence intensity of the control, whereas the blue pepsin-AuNCs retained approximately 80% fluorescence intensity of the

control (see Fig. 5). These data indicate the greater thermal stability of the blue pepsin-AuNCs when exposed to higher temperatures for 30 min, suggesting that a larger size (greater number of aa) protein template and an increased number of protein molecules required to cover the surface of the cluster (larger cluster) may be a source of thermal instability for the protein-AuNCs conjugates.

To investigate if any fluorescence intensity lost after thermal denaturation could be regained by refolding, the P-AuNCs were allowed to recover at RT for 2 h. Fluorescence measurements of the recovered samples revealed that fluorescence lost due to thermal denaturation could not be regained (data not shown).

4. Conclusion

The photophysical and physiochemical properties of P-AuNCs in solution and in dried form are important for their use in a variety of sensing, imaging, and electronic applications. The data presented here show the BSA-AuNCs and green pepsin-AuNCs exhibited resistance to photobleaching under constant UV irradiation, and retained approximately 60% and approximately 50% of initial fluorescence intensity, respectively, after 24-h exposure. The blue pepsin-AuNCs were not as photostable and retained only approximately 10% of initial fluorescence intensity after 24-h UV exposure, possibly due to incomplete coverage of the Au atoms on the surface by the protein molecules. Interestingly, the blue pepsin-AuNCs exhibited the greatest thermal stability, retaining approximately 80% of the control fluorescence intensity after 30-min incubation at 100 °C. In comparison, the BSA-AuNCs retained approximately 5% of the control fluorescent intensity, and the pepsin-Au_{13}NCs lost all fluorescence after 30-min incubation at 80 °C. The high thermal stability of the blue pepsin-AuNCs suggests that a larger protein template and a greater number of protein molecules required to cover the surface of the cluster might be a source of instability for the P-AuNCs. All three synthesized P-AuNCs retained fluorescence in the dried form and exhibited minimal loss (less than 10%) in intensity for a period of up to 6 months when stored at 4 °C. Overall, these results highlight the robustness and long-term stability of the BSA-AuNCs, green pepsin-AuNCs, and blue pepsin-AuNCs, and suggest their potential as attractive materials for an array of bioimaging, sensing, and electronic applications.

5. References

1. Alivisatos AP. Semiconductor clusters, nanocrystals, and quantum dots. Science. 1996;271:933–937.

2. Jiang W, Mardyani S, Fischer H, Chan WCW. Design and characterization of lysine cross-linked mercapto-acid biocompatible quantum dots. Chem Mater. 2006;18:872–878.

3. Kawasaki H, Hamaguchi K, Osaka I, Arakawa R. pH-dependent synthesis of pepsin-mediated gold nanoclusters with blue, green, and red fluorescent emission. Adv Funct Mater. 2011;21:3508–3515.

4. Zhu M, Aikens CM, Hollander FJ, Schatz GC, Jin RJ. Correlating the crystal structure of a thiol-protected Au25 cluster and optical properties. J Am Chem Soc. 2008;130:5883–5885.

5. Baksi A, Xavier PL, Chaudhari K, Goswami N, Pal SK, Pradeep T. Protein-encapsulated gold cluster aggregates: the case of lysozyme. Nanoscale. 2013;5:2009–2016.

6. Chen CT, Chen WJ, Liu CZ, Chang LY, Chen YC. Glutathione-bound gold nanocluster for selective-binding and detection of glutathione s-transferase-fusion proteins from cell lysates. Chem Commun (Camb). 2009;48:7515–7517.

7. Chen H, Li B, Wang C, Zhang X, Cheng Z, Dai X, Zhu R, Gu Y. Characterization of fluorescence probe based on gold nanoclusters for cell and animal imaging. Nanotechnology. 2013;24:055704–055714.

8. Chen WY, Lin JY, Chen WJ, Luo LY, Diau EWG, Chen YC. Functional gold nanoclusters as antimicrobial agents for antibiotic-resistant bacteria. Nanomedicine. 2010;5:755–764.

9. Gerion D, Parak WJ, Williams SC, Zanchet D, Micheel MC, Alivisatos AP. Sorting fluorescent nanocrystals with DNA. J Am Chem Soc. 2002;124:7070–7074.

10. Le Guevel X, Daum N, Schneider M. Synthesis and characterization of human transferrin-stabilized gold nanoclusters. Nanotechnology. 2011;22:275103–27511.

11. Liu TC, Wang JH, Wang HQ, Zhang HL, Zang ZH, Hua XF, Cao YC, Zhao YD, Luo QM. Bioconjugate recognition molecules to quantum dots as tumor probes. J Biomed Mater Res A. 2007;83:1209–1216.

12. Shang L, Dong SJ, Nienhaus GU, Ultra-small fluorescent metal nanoclusters: synthesis and biological applications. Nano Today. 2011;6:401–418.

13. Shang L, Dorlich RM, Brandholt S, Schneider R, Trouillet V, Bruns M, Gerthsen D, Nienhaus GU. Facile preparation of water-soluble fluorescent gold nanoclusters for cellular imaging applications. Nanoscale. 2011;3:2009–2014.

14. Frommer WB, Davidson MW, Campbell RE. Genetically encoded biosensors based on engineered fluorescent proteins. Chem Soc Rev. 2009;38:2833–2841.

15. Medintz IL, Berti L, Pons T, Grimes AG, English DS, Alessandrini A, Facci P, Mattoussi H. A reactive peptidic linker for self-assembling hybrid quantum Dot-DNA bioconjugates. Nano Lett. 2007;7:1741–1748.

16. Qu X, Li Y, Li L, Wang Y, Liang J, Liang J. Fluorescent gold nanoclusters: synthesis and recent biological application. J Nanomaterials. 2015;10:784097–784119.

17. Yong KT, Ding H, Roy I, Law WC, Bergey EJ, Maitra A, Prasad PN. Imaging pancreatic cancer using bioconjugated InP quantum dDots. ACS Nano. 2009;3:502–510.

18. Balasubramanian R, Guo R, Mills AJ, Murray RW. Reaction of $Au_{55}(PPh_3)_{12}Cl_6$ with thiols yields thiolate monolayer protected Au_{75} clusters. J Am Chem Soc. 2005;127:8126–8127.

19. Chen W, Chen S. Oxygen electroreduction catalyzed by gold nanoclusters: strong core size effects. Angew Chem Int Ed. 2009;48:4386–4389.

20. Hussain I, Graham S, Wang Z, Tan B, Sherrington DC, Rannard SP, Cooper AI, Brust M. Size-controlled synthesis of near-monodisperse gold nanoparticles in the 1–4 nm range using polymeric stabilizers. J Am Chem Soc. 2005;127:16398–16399.

21. Negishi Y, Nobusada K, Tsukuda T. Glutathione-protected gold clusters revisited: bridging the gap between gold(I)-thiolate complexes and thiolate-protected gold nanocrystals. J Am Chem Soc. 2005;127:5261–5270.

22. Negishi Y, Takasugi Y, Sato S, Yao H, Kimura K, Tsukuda T. Magic-numbered Au(n) clusters protected by glutathione monolayers (n = 15, 21, 25, 28, 32, 39): isolation and spectroscopic characterization. J Am Chem Soc. 2004;126:6518–6519.

23. Qian H, Zhu M, Lanni E, Zhu Y, Bier ME, Jin R. Conversion of polydisperse Au nanoparticles into monodisperse Au25 nanorods and nanospheres. J Phys Chem C Lett. 2009;113:17599–17603.

24. Rath S, Nozaki S, Palagin D, Matulis V, Ivashkevich O, Maki S. Aqueous-based synthesis of atomic gold clusters: geometry and optical properties. Appl Phys Lett. 2010;97:053103–053105.

25. Yuan X, Yu Y, Yao Q, Zhang Q, Xie J. Fast synthesis of thiolated Au_{25} nanoclusters via protection-deprotection method. J Phys Chem Lett. 2010;3:2310–2314.

26. Zhu M, Lanni E, Garg N, Bier ME, Jin R. Kinetically controlled, high-yield synthesis of Au_{25} clusters. J Am Chem Soc. 2008;130:1138–1139.

27. Xie J, Zheng Y, Ying JY. Protein-directed synthesis of highly fluorescent gold nanoclusters. J Am Chem Soc. 2009;131:888–889.

28. Wei H, Wang Z, Yang L, Tian S, Hou C, Lu Y. Lysozyme-stabilized gold fluorescent cluster: synthesis and application as Hg^{2+} sensor. Analyst. 2010;6:1406–1410.

29. Liu C, Wu H, Hsiao Y, Lai C, Shih C, Peng Y, Tang K, Chang H, Chien Y, Hsiao J, et al. Insulin-directed synthesis of fluorescent gold nanoclusters: preservation of insulin bioactivity and versatility in cell imaging. Angew Chem Int Ed. 2011;50:7056–7060.

30. Wen F, Dong Y, Geng L, Wang S, Zhang S, Zhang X. Horseradish peroxidase functionalized fluorescent gold nanocluster for hydrogen peroxide sensing. Anal Chem. 2011;83:1193–1196.

31. West AL, Griep MH, Cole DP, Karna SP. DNase 1 retains endodeoxyribonuclease activity following gold nanocluster synthesis. Anal Chem. 2014;86:7377–7382.

32. Goncalves MST. Fluorescent labeling of biomolecules with organic probes. Chem Rev. 2009;109:190–212.

33. Hu L, Han S, Parbeen S, Yuan Y, Zhang L, Xu G. Highly sensitive fluorescent detection of trypsin based on BSA-stabilized gold nanoclusters. Biosens Bioelectron. 2012;32:297–299.

34. Hu Y, Guo W, Wei H. Protein- and peptide-directed approaches to fluorescent metal nanoclusters. Isr J Chem. 2015;55:682–697.

35. Wu Z, Jin R. On the ligands role in the fluorescence of gold nanoclusters. Nano Lett. 2010;10:2568–2573.

36. Goldys EM, Sobhan MA. Fluorescence of colloidal gold nanoparticles is controlled by the surface absorbate. Adv Funct Mater. 2012;22:1906–1913.

37. Rosi NL, Mirkin CA. Nanostructures in biodiagnostics. Chem Rev. 2005;105:1547–1562.

38. Xu Y, Sherwood J, Qin Y, Crowley D, Bonizzoni M, Bao Y. The role of protein characteristics in the formation and fluorescence of Au nanoclusters. Nanoscale. 2014;6:1515–1524.

39. Ohta T, Shibuta M, Tsunoyama H, Negishi Y, Eguchi T, Nakajima A. Size and structure dependence of electronic states in thiolate-protected gold nanoclusters of $Au_{25}(SR)_{18}$, $Au_{38}(SR)_{24}$, and $Au_{144}(SR)_{60.}$ J Phys Chem C. 2013;117:3674–3679.

40. MacDonald MA, Zhang P**.** Site-specific and size-dependent bonding of compositionally precise gold-thiolate nanoparticles from X-ray spectroscopy. J Phys Chem Lett. 2010;1:1821–1825.

41. Soptei B, Nagy LN, Baranyai P, Szabo I, Mezo G, Hudecz F, Bota A. On the selection and design of proteins and peptide derivatives for the production of photoluminescent, red-emitting gold quantum clusters. Gold Bull. 2013;46:195–203.

42. Volden S, Lystvet SM, Halskau O, Glomm WR. Generally applicable procedure for in situ formation of fluorescent protein-gold nanoconstructs. RSC Adv. 2011;2:11704–11711.

43. Gole A, Dash C, Ramakrishnan V, Sainkar SR, Mandale AB, Rao M, Sastry M. Pepsin-gold colloid conjugates: preparation, characterization, and enzymatic activity. Langmuir. 2001;17:1674–1679.

44. Egerton RF, Li P, Malac M. Radiation damage in TEM and SEM. Micron. 2004;35:399–409.

List of Symbols, Abbreviations, and Acronyms

aa	amino acid
ARL	US Army Research Laboratory
Au	gold
AuNC	gold nanocluster
BSA	bovine serum albumin
cys	cysteine
DNAseI	Deoxyribonuclease I
HR	high resolution
HRP	horseradish peroxidase
kDa	kiloDalton
N_2	nitrogen
NaOH	sodium hydroxide
NC	nanocluster
O	oxygen
P-AuNC	protein-templated gold nanocluster
pKa	acid strength
RT	room temperature
Si	silicon
Si/O_2	silicon dioxide
TEM	transmission electron microscopy
UV	ultraviolet
XPS	X-ray photoelectron spectroscopy

1 (PDF)	DEFENSE TECHNICAL INFORMATION CTR DTIC OCA
2 (PDF)	DIR ARL IMAL HRA RECORDS MGMT RDRL DCL TECH LIB
1 (PDF)	GOVT PRINTG OFC A MALHOTRA
3 (PDF)	ARL RDRL WM S P KARNA RDRL WMM C S TEYMORIAN RDRL WMM D A A BUJANDA